Proceedings of the 2003 IEEE International Frequency Control Symposium and PDA Exhibition
Jointly with the 17th European Frequency and Time Forum

PROGRESS IN THE BUILDING OF SAPPHIRE-HELIUM CLOCK AT LPMO

P.Y. Bourgeois[1], Y.Kersalé[1], N.Bazin[1],
J.G.Hartnett[2], M.Chaubet[3], and V.Giordano[1]
[1]Laboratoire de Physique et Métrologie des Oscillateurs, CNRS UPR3203, Besançon, France
[2]School of Physics, University of Western Australia, Crawley, Australia
[3]Centre National des Etudes Spatiales, Toulouse, France
Email: pierre-yves.bourgeois@lpmo.edu

***Abstract*— We report a new high-Q Sapphire Whispering Gallery Mode Resonator to achieve ultra high frequency stability. We propose to excite a sapphire resonator in an opened cavity to suppress number of low order spurious modes. Providing the azimutal order of the choosen Whispering Gallery Mode is high enough, Q-factors better than $2 \cdot 10^8$ have been observed which turns out to be sufficient to reach a high frequency stability. A realization of a $12GHz\ WGH$ sapphire helium oscillator shows a relative frequency instability of $2 \cdot 10^{-14}$ in terms of standard deviation.**

keywords — Sapphire Resonator, Whispering Gallery modes

I. INTRODUCTION

The wide development of radars, telecommunications, time and frequency metrology such as atomic fountain clocks using laser cooling, requires high frequency stability sources. For integration times from $0.1s$ to $1000s$, the best frequency stability performances can only be obtained with cooled sapphire oscillators. The use of Whispering Gallery Modes Resonator (WGMR) excitation technique combined with natural low temperature sensitivity and low loss tangent has already prooved high Q-factors ($> 10^9$ [1]) and frequency instability better than $1 \cdot 10^{-15}$ [2] in terms of standard deviation.

At LPMO, we have undertaken the realization of a cryogenic sapphire clock with the support of the french Space and Metrology agencies, *i.e.* the CNES and the BNM. The first objective we set at the beginning of this study is to reach a frequency instability better than $5 \cdot 10^{-14}$ between $1s$ and $10s$. Such a performance enables to qualify the new generation quartz Ultra Stable Oscillators required for space applications. This paper describes the achievement of this preliminary objective. Eventually, this study is the first step in the achievement of an ultra-stable reference oscillator presenting frequency instability better than $1 \cdot 10^{-14}$.

We first describe our resonator design characterized by an original "opened cavity" structure yielding to an efficient spurious modes suppression effect.

Then the oscillator loop design is presented with the first frequency stability measurements.

II. SAPPHIRE RESONATOR DESIGN

The heart of the cryogenic sapphire clock consists in a low defect Al_2O_3 single crystal c-axis oriented rod. For X-band operation, our resonator is $50mm$ diameter and $20mm$ high. As sapphire presents ultra-low dielectric losses, especially at low temperatures, the resonator is charactrized by a high Q-factor providing the electromagnetic field is confined in the rod. This confinement is achieved thanks to the use of a high order Whispering Gallery Mode [3]. In this configuration, electromagnetic energy is essentially located in the rod near the air-dielectric interface. No field stands in the center of the rod then it can be drilled to enable a rigid mechanical mounting (Fig. 1).

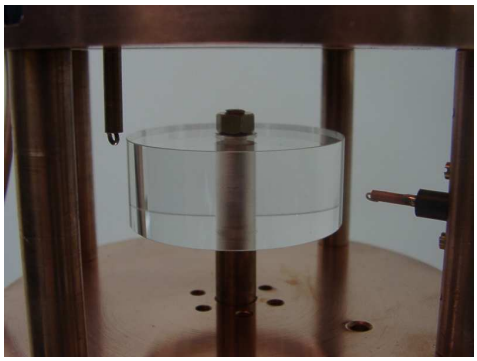

Fig. 1. representation of crystal sapphire

The presence of a small amount of paramagnetic impurities (like Mo^{3+}) modifies the intrinsic frequency temperature dependance yielding to null the temperature sensitivity at a temperature of the order of $6K$.

Although the electromagnetic field is very well confined inside the dielectric rod, the sapphire resonator is generally enclosed in a metallic cavity. This cavity can be made in copper or niobium. It prevents radiation losses and sapphire surface contamination and then enables to achieve very high Q-factors. Moreover it enables an easy mounting of the coupling probes.

Nevertheless, in such a structure, high-Q WGM are embedded in a dense region of low-Q spurious resonance corresponding to the empty cavity modes. These spurious modes can induce Q-factor degradation and thermal sensitivity enhancement of the main resonance. Some techniques like modal selection have already been tested [4], but induce detrimental extral losses at low temperatures. We then propose an "opened

0-7803-7688-9/03/$17.00 © 2003 IEEE

cavity" structure where the cylindrical wall is removed (Fig. 2) and replaced by a microwave absorber.

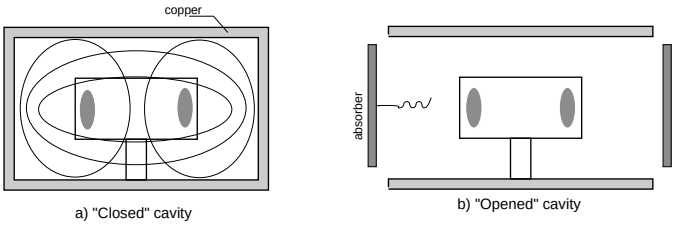

Fig. 2. Comparison between different cavity structures

Spurious modes that are not confined in the rod are then suppressed. On the contrary high order WGM presenting low radiation losses are not drastically affected by the presence of the microwave absorber.

The resonator structure, presented in Fig.3, consist in the sapphire crystal maintained on an OFHC copper 'cold-finger' to ensure thermal contact with the stainless steel can. Thermal sensor and heater are placed in the cold-finger for thermal control and regulation. The axial dimension of the resonant structure is limited by two copper lids placed at 20mm of the sapphire surfaces. The upper lid is fixed on the cold finger whereas the bottom one is maintained by four 10mm diameter copper posts. In addition, one of these copper posts is used to anchor a magnetic loop which generates an azimutal magnetic field H_φ.

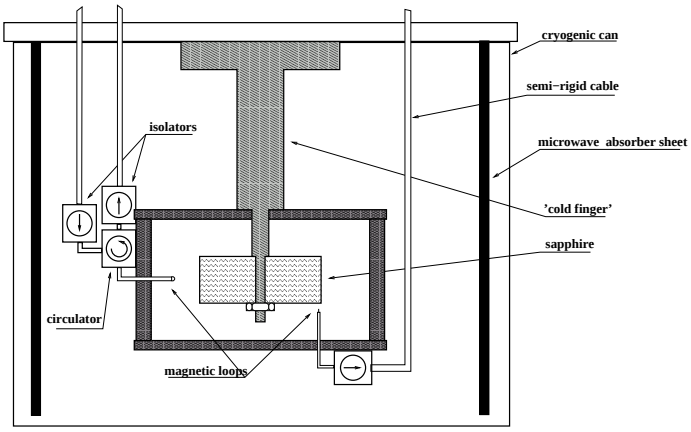

Fig. 3. Schematics of the cryogenic insert

A second magnetic probe anchored in the bottom lid excites a radial magnetic field H_ρ. In order to set the 50Ω reference plans, a circulator and 3 isolators are placed in the crystal's vicinity. All these components are inside the stainless steel cryogenic can whose internal walls are covered with microwave absorber sheets. The cryogenic can is plunged into a large liquid helium dewar.

Microwave 50Ω adapted copper cables around 1.5m long are used to connect the cryogenic resonator structure and the outside room temperature oscillator loop. The choice of this kind of cables instead of stainless steel microwave cryogenic cables limits the signal losses without degrading drastically the thermal insulation of the helium bath.

The cryogenic structure is preliminary cooled down to 77K (liquid nitrogen). The utility of LN_2 is twice. It permits first to reduce helium evaporation during 4.2K cooling. Secondly, we can get good predictions for the future doing measurements on resonator modes at 77K.

The main difficulty to achieve good resonator characteristics is the resonator coupling adjustement. Ideally, the input coupling β1 has to be set to the unity whereas the output coupling β2 to a small value ($\beta 2 \approx 0$) compatible with the sustaining amplifier gain. These values ($\beta 1 \approx 1$ and $\beta 2 \approx 0$) optimize both the resonator loaded Q-factor and the Pound servo operation (see section III). Coupling adjustements have to be done at room temperature before cooling, by observing the reflection coefficient at each resonator port. As the resonator losses drastically decrease between 300K down to 4.2K, coupling factors are generally 4 or 5 orders of magnitude higher at helium temperature than at room temperature. In such a condition, the

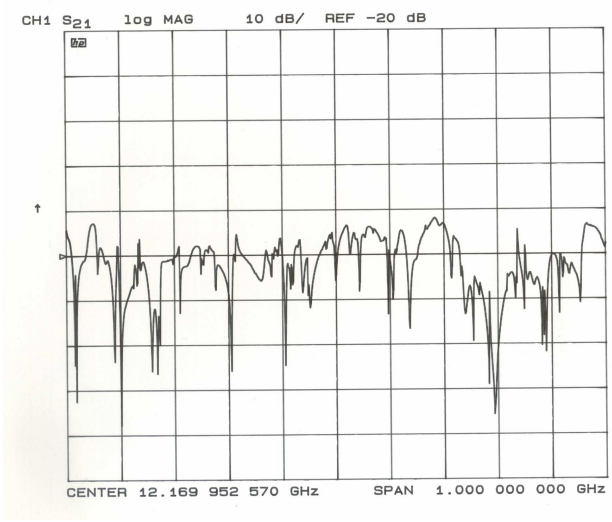

Fig. 4. Frequency configuration on a 1GHz span for a closed cavity $WGH_{17,0,0}$ mode

reflection coefficient observed at room temperature, around the choosen mode frequency, is very close to the unity. Actually we have to detect a small bump 0.01dB deep which is close to the network analyser resolution. Moreover, in the presence of a large number of low-Q spurious resonance, it is impossible to reach such a resolution. From this point of view, the opened cavity stands for a good solution by suppressing most part of the spurious modes. It is demonstrated, by observing the transmission coefficient of the resonator around the 4.2K $WGH_{17,0,0}$ resonance (Fig.4 and 5). In a classical closed cavity (Fig.4), the main resonance is surimposed to a transmission background of the order of $-20dB$. In the opened cavity, this backgroung is less than $-50dB$ which greatly improves the visibility of the main resonance (Fig.5).

The procedure we use consists of approaching the loops in order to achieve greater than required coupling values.

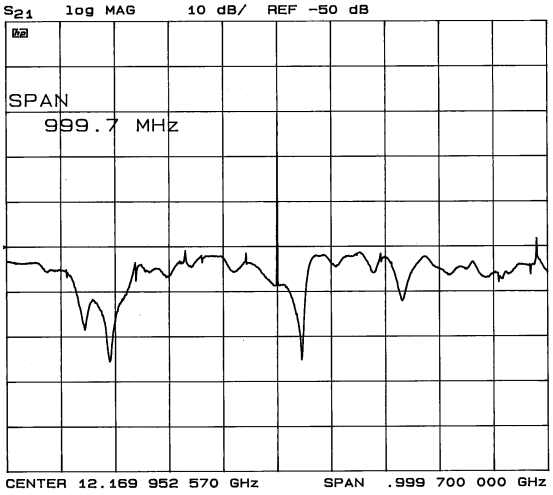

Fig. 5. Frequency configuration on a $1GHz$ span for an opened cavity $WGH_{17,0,0}$ mode

Transmission and reflection coefficients can be then measured with the network analyser. The relative angular position of the probes is adjusted to maximize the transmission signal at resonance. Eventually the probes are moved away to reach the selected coupling values. However, inside the real single crystal, two polarisations of the electromagnetic field coexist [5]. The presence of microscopic defects induces a degeneration of the resonant frequency which forms 2 very nearby modes with only few kHz separation. Unfortunately, at room temperature, these two modes are not discernibles due to the low value of the Q-factor. Then, the preceeding procedure is not able to select only one polarisation. In most cases, the two polarisations are present with equivalent amplitude in the spectrum after the first cool down to $77K$. At this step, a warm-up is necessary to achieve a fine adjustement by rotating one of the probes by a small amount.

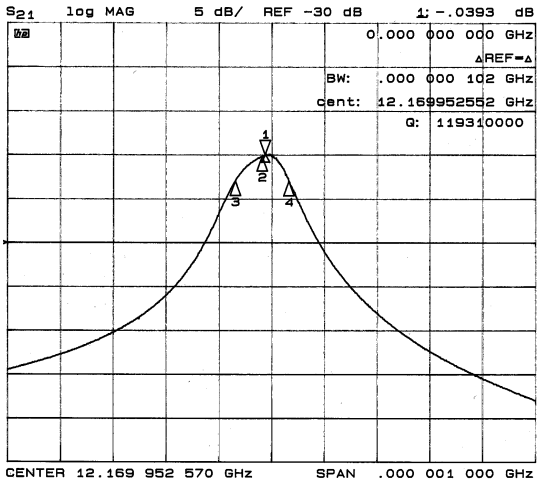

Fig. 6. $WGH_{17,0,0}$ mode frequency and Q-factor at 6K

Figure 6 shows the transmission spectrum around the $WGH_{17,0,0}$ mode at $6K$. The loaded Q-factor is $120 \cdot 10^6$ and the coupling coefficients are $\beta 1 = 1.14$ and $\beta 2 < 0.02$. Unloaded Q-factor ($250 \cdot 10^6$) is lower than some other published results. It should be noted that we observed higher Q values of the order of $500 \cdot 10^6$ in other preliminary experiments. Then the actual limitation could be due to residual radiation losses to some extra losses induced by non perfect coupling probe. Moreover, the shape of the resonance is disturbed by the degeneration of the mode. The two polarisations are only separated by $100Hz$ for this mode. Nevertheless we choose this mode as the oscillator frequency determining element due to the nearby optimised coupling values.

The resonant frequencies of the crystal have been predicted with computational method, using the mode matching technique [6]. The model has been initially developped for a closed cavity configuration. In order to simulate an "opened cavity", we just consider a closed cavity with cylindrical metallic walls standing very far from the sapphire piece. We are aware that this crude assumption limits the accuracy of the model especially concerning the Q-factor because radiation losses are not beeing taken into account. Nevertheless, calculated mode frequencies fit quite well with the experimental observations as demonstrated in table (I).

Indeed, descrepancies are of the order of 1%.

m	computed freq. (GHz)	measured freq. (GHz)
6	5.4705	5.5084
7	6.0820	6.1098
8	6.6941	6.7139
9	7.3060	7.3193
10	7.9174	7.9259
11	8.5282	8.5330
12	9.1382	9.1401
13	9.7475	9.7470
14	10.3561	10.3535
15	10.9638	10.9595
16	11.5707	11.5650
17	12.1769	12.1699
18	12.7823	12.7742
19	13.3870	13.3778
20	13.9910	13.9809
21	14.5942	14.5833
22	15.1968	15.1850

TABLE I

COMPUTED AND MEASURED FREQUENCIES VERSUS AZIMUTAL VARIATION

III. OSCILLATOR LOOP DESIGN

A. Principle

The oscillator loop is composed of one commercial-type $AsGa$ $30dB$ gain amplifier sufficient to compensate the electric losses, a bandpass filter centered in the main resonance, a $10dB$ coupler to derive the output signal by a few dBm and a mechanical phase shifter to satisfy phase condition.

Several isolators are placed in the loop in order to avoid spurious reflections.

It is necessary to supplement the sustaining loop with additional servo devices. Indeed, the link cables joining the resonator structure ($4K$) to electronic loop circuitry ($300K$)

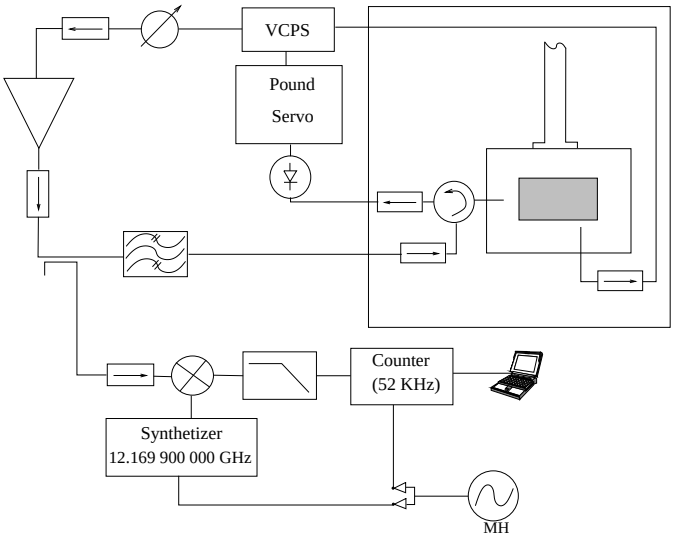

Fig. 7. Schematics of the 6*K* oscillator

undergo large temperature gradients. On top of that, as the liquid helium is evaporating at the speed of $0.4l/h$, the level in the cryostat is falling, and the link cables are then always changing their electrical length, creating thus large phase rotations all along the time. This greatly limits the achievable frequency stability. We evaluate frequency fluctuations due to phase fluctuations up to $\frac{1}{\Delta T}\frac{\Delta\nu}{\nu} \approx 3\cdot 10^{-12}K^{-1}$.

A Voltage Control Phase Shifter (*VCPS*) is then useful for the phase locking (servo Pound [7]).

B. measurements

In order to stabilized the oscillator at the good temperature inversion, we realize several series of temperature ramping at the speed of $0.1K/min$. We then fit the data, and evaluate the mean temperature inversion : $6.0028K$, as shown in Fig. 8.

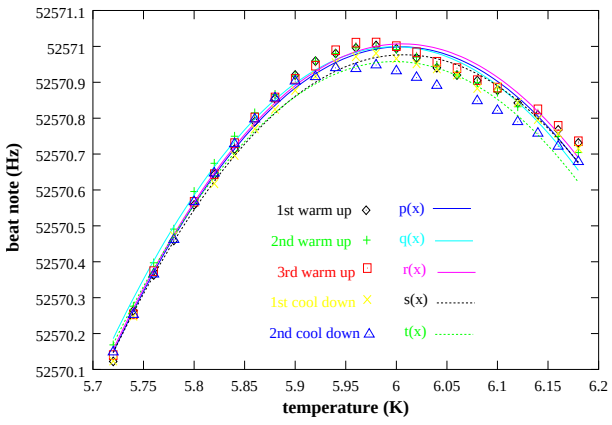

Fig. 8. Determination of the inversion point

The cryogenic oscillator frequency is then compared with a signal delivered by a microwave synthetizer locked on the $10MHz$ hydrogen maser reference signal. The hydrogen maser is placed in a nearby laboratory, the signal is transfered by an optical link without any degradation of the metrological qualities. This system benefits of a relative frequency instability around $2\cdot 10^{-13}$ on $1s$ to better than $5\cdot 10^{-15}$ on $100s$ and more. It is worth noting that no aberrant point has been removed from entire data set recorded over a period of 3 days before the Allan variance computation. Measured standard deviation is then presented in Fig.9. For small integration times ($\tau \leq 10s$), the measurement is limited by the fluctuations of the hydrogen maser. We can observe, between $10s$ and $100s$, a relative frequency instability better than $2\cdot 10^{-14}$.

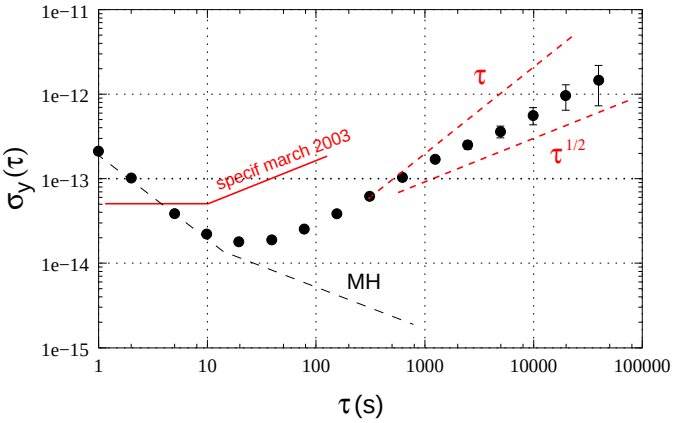

Fig. 9. Allan variance for the oscillator

For long integration times, the standard deviation increases at a rate near $\tau^{1/2}$ which corresponds to a random walk process. Over one day, $\sigma_y(\tau)$ is of the order of $3\cdot 10^{-12}$.

Many causes could explain the long term fluctuations. These can be due to servo Pound dysfunction : presence of AM modulation, isolation fault (only one isolator for each access), the low gain of the integrator. Other causes like the resonator ageing due to the multiple cool down and mechanical contractions can increase the frequency instabillity. But at such a step of our realization, the most critical parameter seems to be the power injected into the resonator.

Indeed, we measured the sensibility of the resonator to the injected power, inserting into the sustaining loop, next to the bandpass filter, a step attenuator and a $20dB$ coupler. This last component derives an output signal injected to a powermeter probe for measuring the actual injected power.

As the servo Pound is working, we can assume the phase fluctuations are controlled and then the observed frequency variations can be only attributed to the change of power. The frequency variation *vs* power is presented in Fig. 10

The resonator sensitivity to the injected power appears linear at around $519Hz/W$, thus relatively to the oscillating frequency (*i.e.* $12.169GHz$) :

$$\frac{1}{\Delta P}\frac{\Delta\nu}{\nu} = 4.3\times 10^{-11}/mW$$

In our oscillator, the power is only stabilized thanks to the loop amplifier saturation. The exact operating point depends on the non-linear amplifier parameters which in turn could be correlated to environemental factors room temperature.

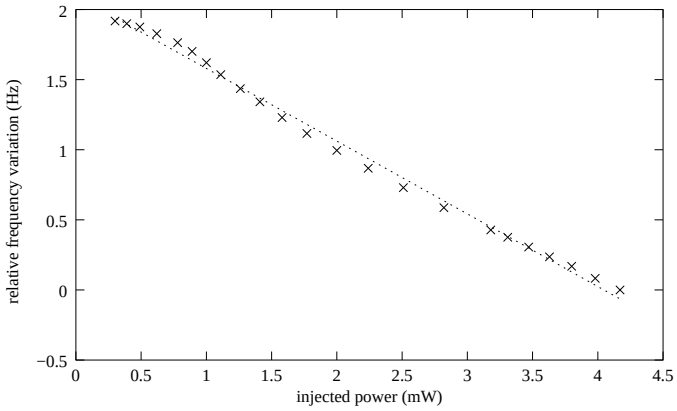

Fig. 10. Oscillating frequency sensitivity *vs* resonator injected power

Moreover the losses along the cryogenic cables are varying during the evaporation, then changing the power injected into the resonator. The next step in our realization is to implement a power servo loop.

IV. Application

Fig. 11 shows as an application the comparison between cryogenic oscillator and a $5MHz$ OSA-type ultra-stable quartz oscillator in order to measure its relative frequency instability.

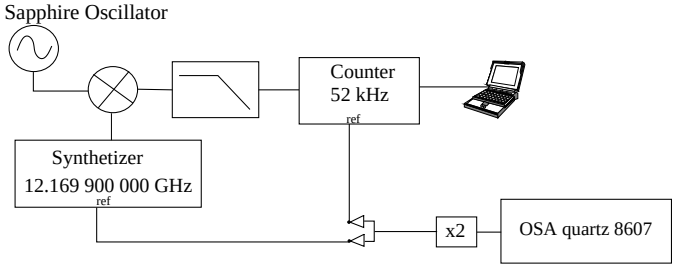

Fig. 11. Measure of OSA 8607 frequency instability

The sapphire cryogenic oscillator appears to be able to resolve frequency instabilities below $7 \cdot 10^{-14}$ for integration times up to 100s. The characterization of the OSA-quartz, presented in Fig. 12, is limited for short term ($\tau = 1s$) by the intrisic noise of the HP synthetizer that has been evaluated elsewhere.

V. Conclusion

We have demonstrated a preliminary result of frequency instability better than $2 \cdot 10^{-14}$ for integration time up to 100s in the building of a sapphire helium clock.

The frequency performances fulfills the requirement for the qualification test of newly developped quartz USO.

In a next step we plan to implement a power servo loop, and to improve thermal control. The problems of resonator coupling have also to be adressed in order to ensure the reproductibility of resonator performances along multiple coolings.

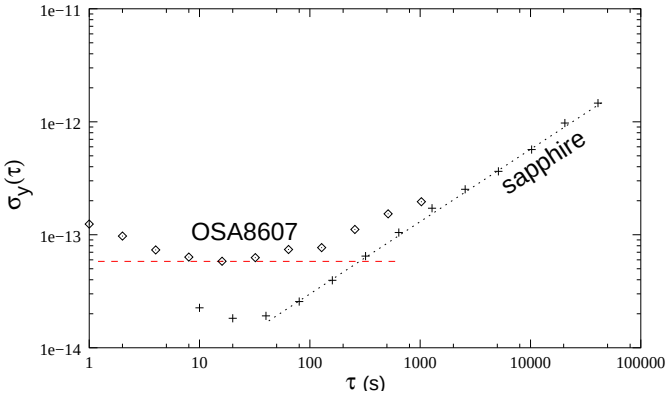

Fig. 12. Measure of OSA 8607 frequency instability

Acknowledgment

This work is supported by the centre national des études spatiales (CNES) and the bureau national de métrologie (BNM). A collaboration with University of Western Australia is also integrated in our works .

References

[1] M.E. Tobar and A.G. Mann, *Resonant frequencies of higher order modes in cylindrical anisotropic dielectric resonators*, IEEE Trans. Microwave Theory Tech, vol. 39, pp. 2077-2083, 1991.

[2] S. Chang, A.G. Mann and A.N. Luiten, *Improved cryogenic sapphire oscillator with exceptionally high frequency stability*, Electronic Letters,vol. 36, pp. 480-481, 2 2000.

[3] V.F. Vzyatyshev, V.I. Kalinichev, V.I. Kuimovi *Physical Phenomena in a Cylindrical Metal-Dielectric Resonator and the Problems Associated with designing screened dielectric resonators*, Radiotekhnica i elektronika, n 4, pp. 705-712, 1985.

[4] O. Di Monaco, W. Daniau, I. Lajoie, Y. Gruson, M. Chambet and V. Giordano *Modal selection for a whispering gallery mode resonator*, Electronics Letters, vol. 32, n7, pp. 669-670, 28th march 1996.

[5] O. Di Monaco, Y. Kersalé and V. Giordano *Resonance Degeneration and Spurious Mode Suppression in a Cryogenic Whispering Gallery Mode Sapphire Resonator*, IEEE Microwave and Guided Wave Letters, vol. 10, n9, pp. 368-370, sept. 2000

[6] E.N Ivanov, D.G. Blair, V.I. Kalinichev *Approximate approach to the design of shielded dielectric disk resonators with whispering-Gallery Mode*, IEEE MTT, vol. 41, n 4, pp. 632-638, april 1993.

[7] A.N. Luiten, A.G. Mann, M.E. Costa and D.G. Blair *Power Stabilized Cryogenic Sapphire Oscillator* IEEE IM, vol. 44, n 2, pp. 132-135, april 1995